NATURALISTA CAMPANO
ISSN: 1827-7160
Volume 28 Issue 1, 2024

A Systematic Study on the Structural, Electrical and Optical Behavior of Rare Earth Doped Strontium Oxide Nanophosphors

J. B. Reshmi[1], S. Grace Victoria[2*]

[1]Research Scholar, Department of Physics & Research Centre, Women's Christian College, Nagercoil, Tamil Nadu, India
Affiliated to Manonmaniam Sundaranar University, Abishekapatti, Tirunelveli, Tamil Nadu, India
[2]Assistant Professor, Department of Physics & Research Centre, Women's Christian College, Nagercoil, Tamil Nadu, India
Affiliated to Manonmaniam Sundaranar University, Abishekapatti, Tirunelveli, Tamil Nadu, India
Corresponding Email: sujienthersally@gmail.com

Abstract: The primary aim of the present work is to synthesize SrO nanoparticles employing the sol-gel process and then to effectively add lanthanum in different proportions and study its effect on the properties. The crystalline makeup, dimensions and morphological structure of the nanopowders were scrutinized using state-of-the-art techniques such as X-ray diffraction (XRD), Fourier-transform infrared spectroscopy (FTIR), Scanning electron microscopy (SEM) with energy-dispersive X-ray analysis (EDAX), Ultraviolet-visible spectroscopy, Impedance measurement and photoluminescence (PL) spectral analysis. The nanoparticles' well-defined crystalline structure is distinctly visible in the XRD patterns. Crystalline size is found to be around 70 nm. The morphology and purity of the synthesized sample were validated by SEM and EDAX scans of the surface. Impedance study denotes the low resistance and high conductivity of the produced lanthanum doped SrO sample which offers a consistent electrochemical setting that is well-suited for optoelectronic application. The higher concentration of La (3%) appears to have a considerable impact on the excited states, resulting in a longer average lifetime. Lifetime values are in the order of nano second enabling these phosphors to be applied in lighting and display devices.

Keywords: Rare earth metal, SrO, XRD, SEM, EDAX, FTIR, UV-visible, Impedance, PL.

1. Introduction

Numerous scientific and technological sectors have been transformed by nanotechnology, which has produced innovative materials with distinctive features and uses. With their unique characteristics and potential uses, nanoparticles have become a crucial area of study for many different branches of science. One such exceptional nanomaterial that has drawn a lot of interest because of its interesting features and wide range of uses is SrO NPs. [1]. Strontium is an alkaline earth metal that occurs naturally [2]. It may form oxides with various oxidation states. SrO is of special significance because of the wide range of industries it is used in, including biomedicine, electronics, sensing, catalysis and environmental remediation [3]. It explores their uses in disciplines like catalysis, biomedicine, sensing, electronics and environmental remediation while identifying promising directions for additional study and advancement [4].
In recent years, rare earth (RE) doped nanomaterials has attracted wide use in various applications as thin film electroluminescent (TFEL) devices, optoelectronic or cathodoluminescent devices. RE-doped insulators are used in telecommunications, lasers and amplifiers, medical analysis and phosphors, etc. Generally rare earth doped aluminates have greater impact on defect centres within the band gap. The emission of light from the ultraviolet, visible, and Infrared depends on the host material properties [5].The key to this doping method is the precise regulation of dopant concentrations, which directly determines the overall performance of the LED device [6]. The inclusion of La, for example, must achieve a careful equilibrium between enhancing charge transfer and preventing harmful consequences resulting from excessive doping.Moreover, the interaction between these additives goes beyond their individual effects, resulting in synergistic outcomes that enhance the overall efficiency of the LED. This optimizes the circumstances for effective charge injection, transport, and recombination, resulting in improved LED brightness [7]. The incorporation of these scarce earth elements into

metal oxides not only advances the current level of LED technology, but also offers great potential for future advancements in lighting, displays and optoelectronics.

2. Experimental

Materials

99% Strontium nitrate (AR Grade) is utilised as the precursor and 99% pure NaOH is chosen as the reagent to synthesize SrO nanoparticles (NPs). Lanthanum (III) Nitrate hexahydrate (AR Grade) is utilised as dopant. Solutions are prepared in freshly prepared deionized water. The compounds were used without any further processing.

Preparation of lanthanum doped SrO NPs

Sol gel method is used to prepare the sample which is simple and cost effective. All reagents used in the synthesis were analytical grade and used without further purification. 0.5M Strontium nitrate was dissolved in 250 ml of distilled water and 0.5 M of sodium hydroxide was added drop wise. A white precipitate appeared in the beaker. Fine powders were seen to be deposited. It was filtered using filter paper and kept for 2-3 days to dry. The dried fine powder is utilised for further analysis.In order to prepare a sol, 26g of strontium nitrate was dissolved in 250 ml of distilled water and 5 g of sodium hydroxide was dissolved in 250 ml of distilled water. The solutions were stirred with constant stirring for about five minutes each. 0.108 g of lanthanum nitrate (**Lanthanum 1%)** was added to the solution containing strontium nitrate. Sodium hydroxide solution was added drop wise. A white precipitate appeared in the beaker. Fine powders were seen to be deposited. It was filtered using filter paper and kept for 2-3 days to dry. The dried fine powder is utilised for further analysis. The percentage of Lanthanum was varied to **Lanthanum 2 % (**0.216g of lanthanum nitrate) and Lanthanum **3% (**0.324g of lanthanum nitrate) to study the effect on the properties.

Characterization techniques

The material characterization of the SrO nanoparticles (NPs) was carried out using an Analytical X-Ray Diffractometer (sample stage 3071/xx) with copper target (λ = 1.5405 A˚) in theta and 2 theta scan modethat allowed for precise X-ray diffraction analysis. This analysis provided valuable information about the crystalline structure and phase composition of the synthesized SrO NPs. FTIR analysis was performed on FTIR spectrophotometer (Thermo Nicolet 380 FTIR spectrophotometer) and the wavelength range is from 4000 to 400$cm^{-1.}$ This spectroscopic technique is highly effective in detecting the vibrations of atoms and molecules within the material, helping to identify specific chemical bonds and functional groups. For SEM analysis model Jeol JSM6390were used. The optical properties of the deposited samples were analysed by UV-DRS spectrophotometer. This evaluation involved studyingtheir absorbance and transmission characteristics, providing insights into the material's behaviourwith respect to light.The photoluminescence spectra were performed by the cary eclipse instrument.This photoluminescence analysis allowed for the investigation of the light emission behaviour of the nanoparticles, shedding light on their potential for applications in optoelectronics and other luminescent devices.

3. Result and Discussion

XRD ANALYSIS

X-Ray Diffraction of SrO: La

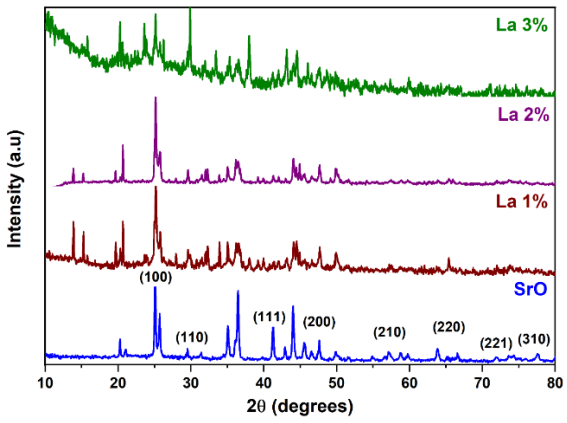

Figure 1. XRD pattern of SrO doped Lanthanum

XRD analysis was conducted to identify the crystalline nature of the synthesised SrO nanopowder.The X-ray diffraction (XRD) measurements revealed valuable insights into the crystal phase andpurity of the synthesized SrO nanopowder. As depicted in Fig. 1, the XRD pattern ofstrontium oxide nanoparticles produced using NaOH as the precipitant exhibited distinct peaks at25.0° (100), 32.0° (110), 42° (111), 46.0° (200), 57.5° (210), 58.5° (211), 64.0° (220), 72° (221)and 78.0° (310) degrees, indicating the presence of prominent prospective crystal planes [22]. To ascertain theidentity of these diffraction peaks, a comparison was made with the reference data from theJCPDS No 01-073-0661 database. Crystalline size is found to be 42 nm.Crystallite size of SrO is calculated using Debye Scherrer's formula

$$\boldsymbol{D = \frac{k\lambda}{\beta \cos \theta}} \quad (1)$$

where k is the shape factor (0.9), λ is the wavelength of the X- ray, β is full with and half maxima, and θ is the angle of the diffraction. Well defined and sharp diffraction peaks show the single crystal nature of the grown samples [8].

Lanthanum oxides has three dominant peaks at 2θ values 28.1, 39.7, 48.7º respectively. When lanthanum is introduced as a dopant into strontium oxide (SrO: La), the XRD pattern undergoes noticeable alterations. The particle size obtained is 77 nm, 72 nm and 70 nm. The sharp peak indicates that nanoparticles are well crystallized [11]. The peak intensities decrease with the increase in doping concentrations, which indicates that an increase in doping concentration deteriorates the crystallinity of the nano particles. This indicates the impregnation of the dopant ions into the lattice replacing Sr^{2+} the ions. Ionic radius of dopant ion (La^{3+}= 1.36 Å) islarger compared to the native ion (Sr^{2+} =1.18 Å),dopant ions occupy the places of Sr^{2+} ions without much difficulty. These observations further suggest that the present doping level of rare earth ions in strontium oxide lattice not completely collapse the crystal structure of host material.

Fourier Transform Infrared Spectroscopy (FT-IR) of SrO: La

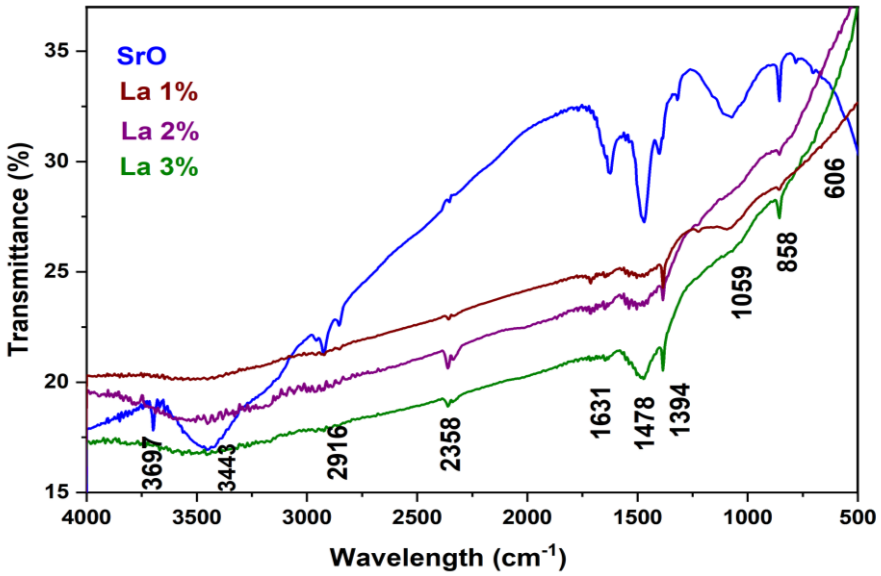

Figure 2. Fourier Transform Infrared Spectroscopy (FT-IR) of SrO: La

The FTIR spectroscopy technique was employed to gain valuable insights into the binding and functional groups present in the SrO nanoparticles shown in figure (2). The functional group in the SrO NPs was determined by employing aFTIR spectrophotometer (Thermo Nicolet 380 FTIR spectrophotometer) and the wavelength range is from 4000 to 500cm^{-1}.One of the notable peaks observed in the FTIR spectrum is located at 858 cm-1, which is attributed to the SrO bond.

The variations of the spectra after doping exhibit only slight modifications on the position but more extensive changes in the intensity of the vibration bands O-'the acetate ligands [12]. The bands in the 2800cm^{-1} to 3000cm^{-1} region are attributable to symmetric arid asymmetric stretching vibration of -CH_3 groups. Other strong bands, produced by -COO- stretching vibrations, were also observed at 1478 cm^{-1} (COO-) and at 1394 cm^{-1} (-COO-).

These are followed by CH_3 bending vibrations, both of which occur between 1400cm^{-1} and 1340 cm^{-1}. CH_3 rocking vibrations were recorded at 1059 cm^{-1}, whereas the C=C stretching vibrations are positioned at 943cm^{-1}. For frequencies lower than 700 cm^{-1}, strong intensities of the fundamental bending vibrations of the rnono carboxilie acid groups (COO) appear at 606 cm^{-1}, respectively [13]. There is slight stretching and rocking vibration bands of $–CH_3$ groups in the 2800 to 3000 cm^{-1} and 1059 to1023 cm^{-1} regions due to poorly bonded acetate species [14].peaks observed at 606cm^{-1} ,1478 cm^{-1} ,1059 cm^{-1}, which can be ascertained to stretching vibration of the La-O bond.

UV-Visble spectroscopy of La doped SrO

UV visible spectroscopy studies on nanoparticles, specifically strontium oxide doped with varying concentrations of lanthanum (La) are of paramount importance in advancing our understanding of nanomaterials and their potential applications [15]. These studies are necessary to explore and enhance the photoluminescent properties of SrO NPs. By doping SrO with 1%, 2%, and 3% of the rare earth elements, researchers can precisely control and fine-tune the optical properties of the nanoparticles. UV visible spectroscopy allows us to investigate the absorption and emission characteristics of these doped nanoparticles, shedding light on the quantum mechanical processes occurring at the nanoscale. Understanding how different dopant concentrations affect the photoluminescent properties is vital for designing materials with tailored optical properties, which have applications in fields like optoelectronics, sensors, and displays [16].

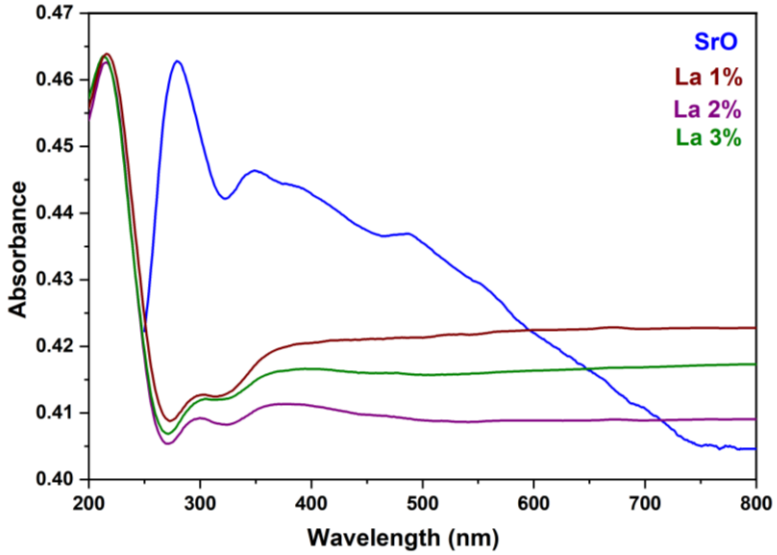

Figure 3. UVVisble spectroscopy of La doped SrO

UV-visible spectroscopy is a powerful analytical technique used to study the electronic transitions in various materials, including metal oxides like strontium oxide (SrO) and lanthanum-doped strontium oxide (SrO: La). When comparing the UV-visible spectroscopy peaks of these two compounds, distinct differences can be observed. In the UV-visible spectrum of strontium oxide (SrO), characteristic peaks are typically found within the ultraviolet region, primarily around 200-400 nm. These peaks result from electronic transitions of the valence electrons to higher energy levels within the crystal lattice[17]. The specific wavelengths and intensities of these peaks can vary depending on factors like crystal structure and impurities, but they typically correspond to the intrinsic electronic properties of SrO.

Figure 3 shows the UV-Vis spectra of SrO: La nanomaterials. As shown in the figure 3spectra SrO: La show a strong light absorbance edge close to 300 nm due to its inherent band gap (~3.4 eV). This displays considerable advancement of visible light reflection, therefore there is betterment in electrochemical reactions by visible light besides ultra-violet. Owing to unique half-filed electronic configuration of La, has the capacity to form new intermediate energy levels inside the band gap of SrO: La and contracts the distance across the valence band and conduction band. The additional state leads to effective red-shift (longer wavelength) of the absorption threshold [18]. The Kubelka-Munk function F(R) is for the most part connected to change over the diffused reflectance into equivalent absorption coefficient and utilized for examining the powders as given by equation (2).

$F(R)= (1 R)^2/(2R)$ (2)

where R: the reflectance, F(R): Kubelka-Munk function. The optical energy gap was calculated using Tauc relation; the band gap (Eg) of semiconductor material can be calculated from equation (3)

$F(R)\ h\nu = A\ (h\nu - Eg)^n$ (6)

where n = 1/2 and 2 for direct and indirect transitions respectively.

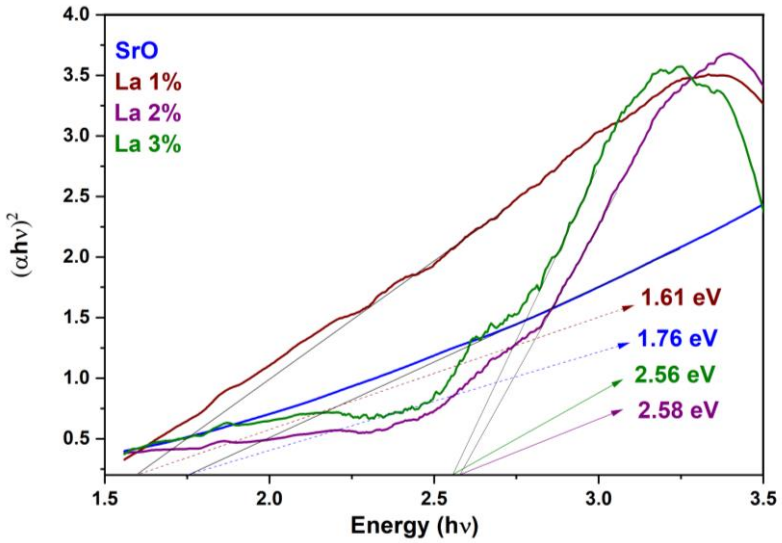

Figure 4 Tauc plot

Tauc relationwas used to calculate optical energy gap thereby given the direct band, as shown in Figure 4.From the Tauc plot perspective, the bandgap of a material is influenced by factors such as the composition and doping concentration. In this case, the addition of lanthanum (La) to strontium oxide (SrO) seems to impact the bandgap energy.The SrO shows bandgap of ~1.76eV, SrO:1%La shows bandgap of ~1.61 eV, SrO:2%La shows bandgap of ~2.58 eV and SrO:3%La shows bandgap of ~2.56 eV. The pure SrO has a bandgap of ~1.76 eV.The addition of 1% La reduces the bandgap to ~1.61 eV.However, as the La concentration increases to 2%, the bandgap significantly increases to ~2.58 eV.At 3% La concentration, the bandgap remains relatively high at ~2.56 eV.This trend suggests that the introduction of lanthanum has a non-linear impact on the bandgap of strontium oxide. The decrease in bandgap with 1% La may be attributed to the influence of La on the electronic structure of SrO. However, the subsequent increase in bandgap with higher La concentrations might be due to complex interactions and changes in the material's properties [19].Understanding and controlling these variations in bandgap are crucial for tailoring the optical and electronic properties of semiconductors, which have implications for applications such as solar cells, photodetectors, and other optoelectronic devices [20].

Scanning Electron Microscopy (SEM) of SrO: La

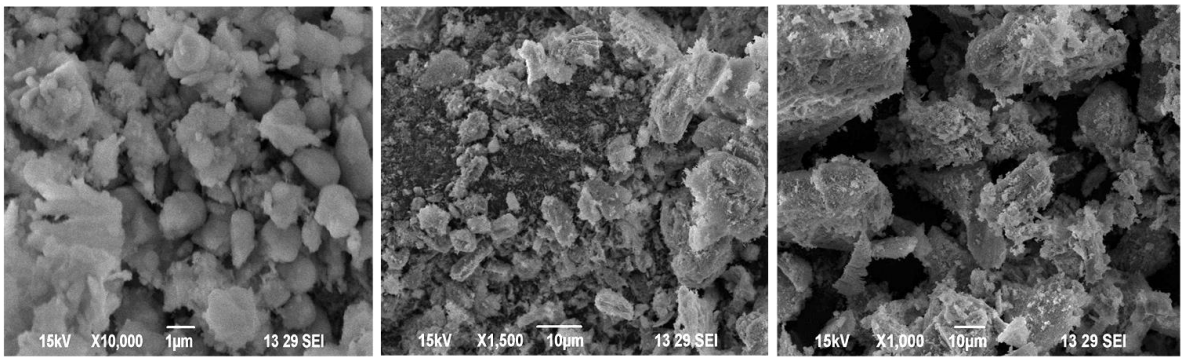

Sro-La(1%) **Sro-La(2%)** **Sro-La(3%)**

Figure 5 SEMof SrO: La

The scanning electron microscopy (SEM) image depicts SrO: La exhibiting a pseudospherical morphology at ambient temperature is shown in Figure 5. The surface morphology was in the form of granular structure with somewhat round shape and were interlinked with each other, leading to the formation of bigger particles [21]. Also, it was found that some irregular aggregations were formed in the image. The morphology was investigated with SEM. The ImageJ software revealed a nanostructure with an average diameter of 60-80 nm for SrO: 1% La, 40-50 nm for SrO: 2% La and 40-60 nm for SrO: 3% La. The material indicating the irregularities in shapes and structures have a very few sugars like shape with narrow size distribution.

Energy-dispersive X-ray spectroscopy (EDS) of SrO: La

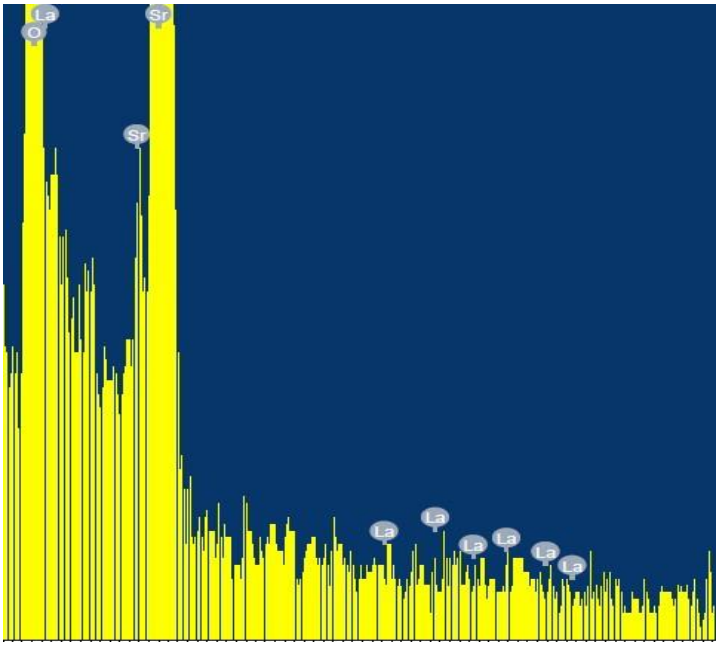

Figure 6a. Sro-La (1%)

Element	Weight%	Atomic weight %
O K	**4.35**	**83.46**
Sr L	**4.79**	**16.74**
La L	**-0.09**	**-0.20**

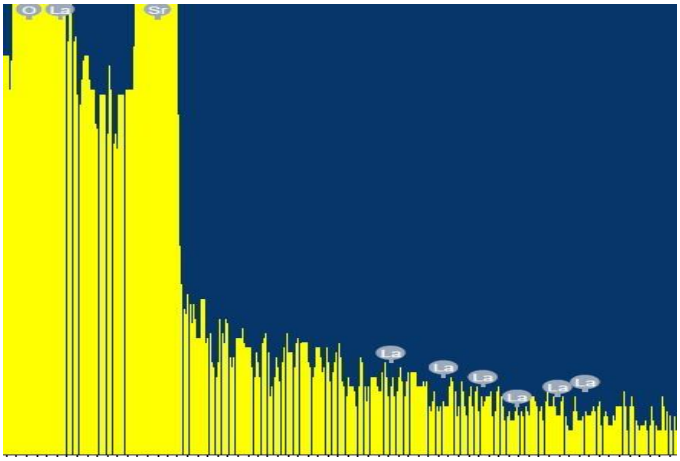

FIGURE 6B Sro-La (2%)

Element	Weight%	Aztomic weight %
O K	**5.58**	**81.24**
Sr L	**7.06**	**18.79**
La L	**-0.02**	**-0.03**

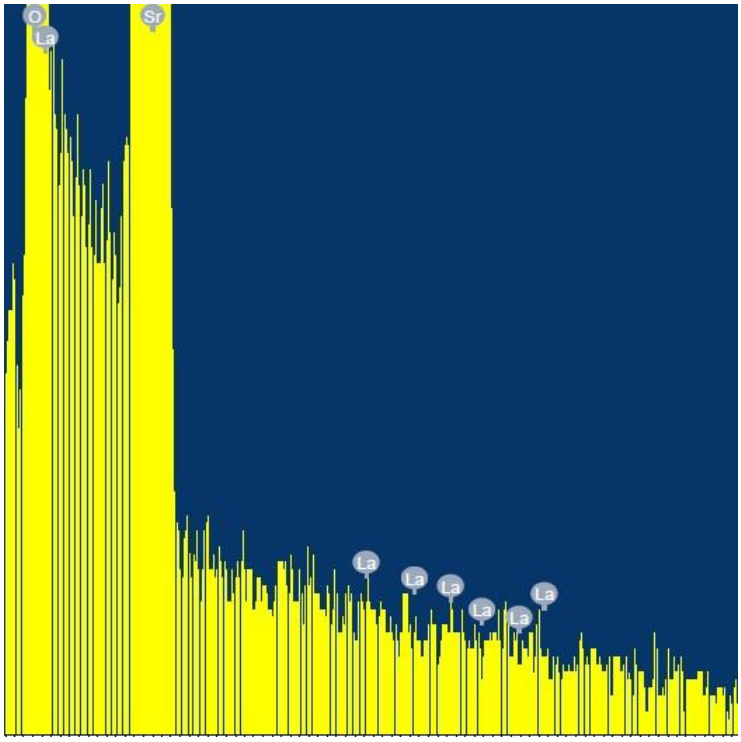

Figure 6c Sro-La(3%)

Element	Weight %	Atomic weight %
O K	8.01	82.24
Sr L	9.49	17.77
La L	-0.01	-0.01

Energy dispersive X-Ray Analysis is an X -ray technique used to identify the elemental composition of materials. The data generated by EDAX analysis consist of spectra showing peaks corresponding to the elements making up the true composition of the sample being analysed. It is also used for the purity check of the prepared samples. Fig 6a,6b,6c shows the EDAX spectra of lanthanum doped strontium oxide nano powders. Recorded spectra have peaks only at the specified locations for the individual elements of Sr, La. And O.

Electrochemical Impedance Spectroscopy (EIS) of SrO: La

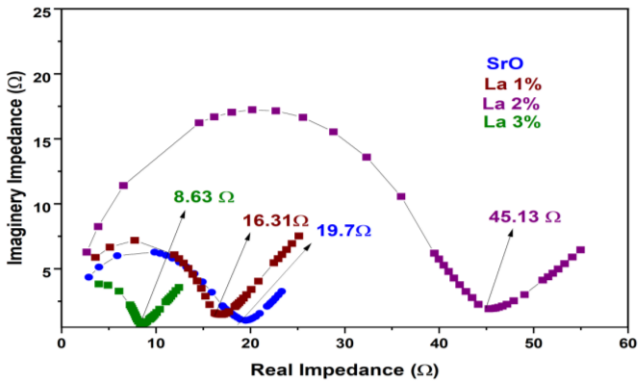

Figure **7.** Electrochemical Impedance Spectroscopy (EIS) of SrO: La

The Nyquist plot obtained from impedance spectroscopy is a valuable tool for analysing the electrochemical characteristics of an electrode, presented in Figure 7.The plot provides insights into the electrical behavior of the material under investigation.The information derived from the plot includes the equivalent series resistance (RS), charge transfer resistance (RCT), and the presence of a Faradaic mechanism of charge storage.The electrode exhibited a very low equivalent series resistance, R_S of 0.48 Ω, which is the combination of ionic resistance, resistance from substrate and contact resistance between the active material and current collector; obtained from the intersection of *x*-axis of the Nyquist plot. Charge transfer resistance, R_{CT} was found to be 19.7 Ω for SrO, R_{CT} was found to be 16.31 Ω for SrO: 1%La, R_{CT} was found to be 45.13 Ω for SrO: 2%La and R_{CT} was found to be 8.63 Ω for SrO:3%La, obtained from the diameter of the semicircle at high frequency region. Charge transfer resistance is an important parameter that indicates the ease or difficulty of charge transfer at the electrode-electrolyte interface[28]. Lower RCT values generally suggest better electrochemical performance. The presence of charge transfer resistance in the Nyquist plot suggests the involvement of a Faradaic mechanism of charge storage. Faradaic processes involve electrochemical reactions that result in the storage or release of charge. This is in contrast to non-Faradaic processes, which do not involve chemical reactions. The identification of a Faradaic mechanism provides important information about the nature of the electrochemical reactions occurring at the electrode[28]. The Nyquist plot and the associated parameters provide a comprehensive understanding of the electrochemical behavior of the electrode material. The low equivalent series resistance, along with the variation in charge transfer resistance for different compositions, indicates the potential of the material for electrochemical applications.Presence of charge transfer suggests the presence of Faradaic mechanism of charge storage [28].

Photoluminescence (PL) of SrO: La

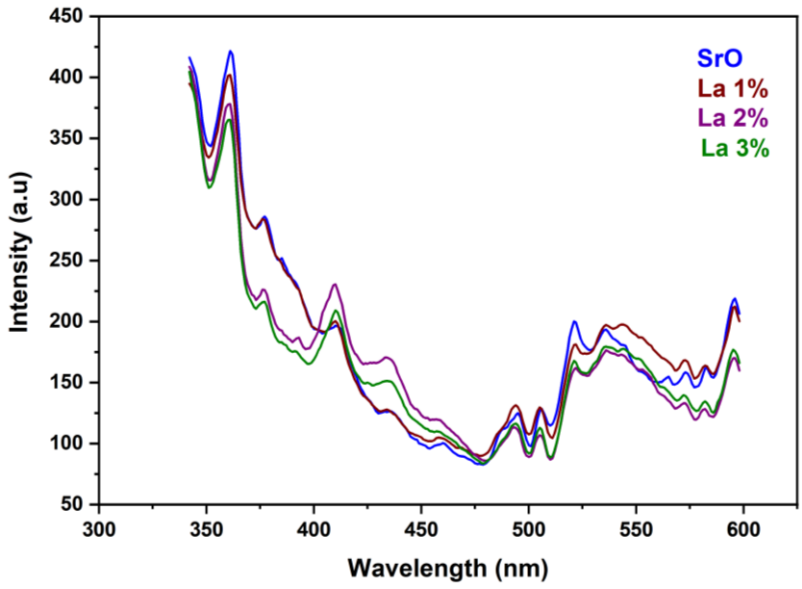

Figure 8: Photoluminescence (PL) spectra of SrO:La

The samples were stimulated with light at a wavelength of 290 nm, corresponding to an energy of 4.27 eV. The PL measurements were conducted throughout a wavelength range of 300 to 600 nm (corresponding to an energy range of 3.1–1.37 eV) with a precision of 1 nm. Rare-earth doped long persistence materials have been widely studied due to their many advantages, such as high luminescent brightness, long afterglow time, good chemical stability, and environmental friendliness. The PL under 360 nm excitation showed three peaks at 395 nm, 520 nm, and 600 nm corresponding to uv, green and IR region of spectrum, respectively. The strong peak showing blue emission at 395 nm was due to the exciton emission, and weak green emission at 520 nm was due to oxygen interstitial. The strong UV emission corresponds to the exciton recombination related near-band edge emission of nanoparticles [21]. The green emissions are possibly due to surface defects in the nanoparticles. La-doped SrO nanophosphors have the remarkable ability to combine two or more low energy photons to generate a single high-energy photon by an anti-Stokes process and hold great promise for a broad range of applications, ranging from high-resolution bio imaging to modern photovoltaic technologies [22]. In contrast to conventional luminescent probes, lanthanide-doped SrO nanophosphors exhibit excellent photo stability, continuous emission capability, and sharp multi-peak line emission. [23].

Lifetime of SrO: La

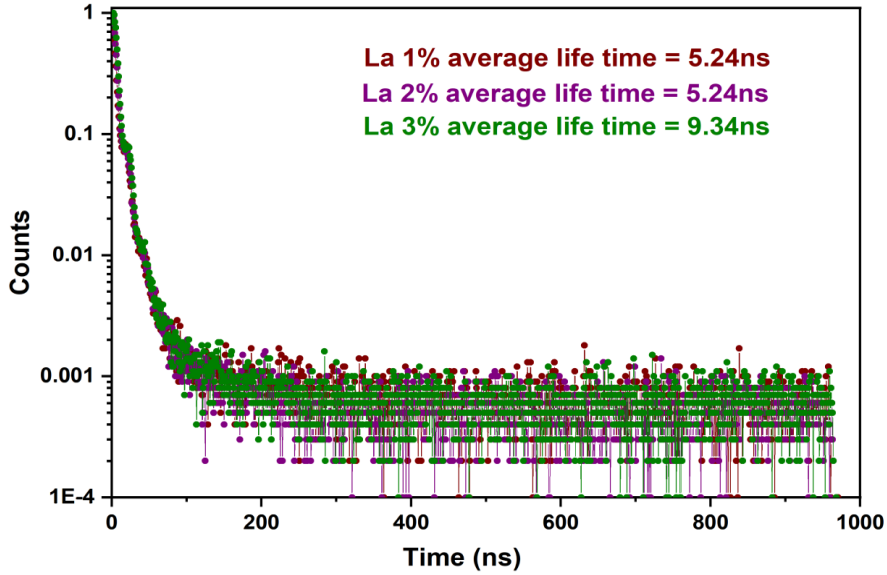

Figure 9 Lifetime of SrO: La

The fluorescence lifetime is a measure of the a fluorophore spends in the excited state before returing to the ground state by emitting a photon.The Figure 9 describes the lifetime spectra of SrO doped with different concentrations of La. The lifetime spectra refer to the average lifetimes of excited states of these materials, which are measured in nanoseconds (ns). The average life time of La 1% doped SrO is 5.24 ns. The average life time of La 2% doped SrO is 5.24 ns.The average life time of La 3% doped SrO is 9.34 ns. The lifetimes for La 1% and La 2% doped SrO are identical at 5.24 ns. This suggests that the addition of 1% or 2% lanthanum does not significantly affect the average lifetime of the excited states in SrO. The significant increase in the average lifetime to 9.34 ns for La 3% doped SrO indicates a notable change in the material's behavior. The higher concentration of La (3%) appears to have a considerable impact on the excited states, resulting in a longer average lifetime. The lifetime might saturate or reach a plateau beyond a certain concentration of lanthanum. In this case, the increase from 1% to 2% did not change the lifetime, but the jump to 3% caused a significant increase. Lanthanum doping could be influencing the energy levels of the excited states, leading to changes in the decay processes and, consequently, the average lifetime[25]. The efficiency of lanthanum incorporation into the SrO lattice may vary with concentration, impacting the material's optical properties.

4. Conclusion

The study examines the properties of La-doped SrO emphasizing its capacity to improve efficiency and performancein light-emitting diodes (LEDs). The XRD examination reveals the presence of highly crystalline nanoparticles with dimensions ranging from 70 to 77 nm. The ImageJ software detects nanostructures measuring 60-80 nm in diameter for SrO: 1% La, 40-50 nm for SrO: 2% La, and 40-60 nm for SrO: 3% La. La-doped SrO nanophosphors exhibit the capacity to convert low-energy photons into high-energy photons through an anti-Stokes process, showing potential for applications such as bioimaging and photovoltaics. The UV spectra of SrO:La show a notable absorption of light at 300 nm due to its band gap of around 3.4 eV. This leads to enhanced reflection of visible light and electrochemical reactions that extend beyond the UV range. The addition of lanthanum is anticipated to have an impact on the energy levels of excited states, which in turn affects the decay processes and average lifespan. Decreased RCT values correspond to enhanced electrochemical performance. In summary, the work highlights the capacity of La-doped SrO to enhance LED technology and its wider range of uses.

5. Reference

1. Rojas-Hernandez, R. E., Rubio-Marcos, F., Rodriguez, M. Á., & Fernandez, J. F. (2018). Long lasting phosphors: $SrAl_2O_4$: Eu, Dy as the most studied material. Renewable and Sustainable Energy Reviews, 81, 2759-2770.
2. Jin, L., Batuk, M., Kirschner, F. K., Lang, F., Blundell, S. J., Hadermann, J., & Hayward, M. A. (2019). Exsolution of SrO during the topochemical conversion of $LaSr_3CoRuO_8$ to the oxyhydride $LaSr_3CoRuO_4H_4$. Inorganic chemistry, 58(21), 14863-14870.
3. Lee, J. W., Singh, S. P., Kim, M., Hong, S. U., Park, W. B., & Sohn, K. S. (2017). Metaheuristics-assisted combinatorial screening of Eu^{2+}-doped Ca–Sr–Ba–Li–Mg–Al–Si–Ge–N compositional space in search of a narrow-band green emitting phosphor and density functional theory calculations. Inorganic Chemistry, 56(16), 9814-9824.
4. Tolhurst, T. M., Braun, C., Schnick, W., &Moewes, A. (2021). Comprehensive band gap and electronic structure investigations of the prominent phosphors $M_2Si_5N_8$: Eu^{2+} (M= Ca, Sr, Ba) determined using soft X-ray spectroscopy and density functional theory. The Journal of Physical Chemistry C, 125(46), 25799-25806.
5. Swathi, B. N., Krushna, B. R., Hariprasad, S. A., Srikanth, C., Subramanian, B., Prasad, B. D., & Nagabhushana, H. (2023). Designing vivid green $Sr_9Al_6O_{18}$: Er^{3+} phosphor for information encryption and nUV excitable cool-white LED applications. Journal of Luminescence, 257, 119618.
6. Sehrawat, P., Boora, P., Kumar, M., Malik, R. K., Khatkar, S. P., &Taxak, V. B. (2020). Crystal structure engineering and optical analysis of novel greenish $Sr_{9-x}Al_6O_{18}$:x Er^{3+} nanomaterials for NUV excitable cool-white LED applications. Chemical Physics Letters, 759, 138044.
7. Stanciu, C., Hau, S., Stanciu, G., Trusca, R., Vasile, B. S., & Tihon, C. (2023). Structural, microstructural characterization and luminescence spectroscopy of europium-doped strontium titanate prepared by the sol-gel method. Ceramics International.
8. Wang, Z., Zhang, M., He, J., Tang, Y., He, T., Sun, Q., ... & Wang, Y. (2021). Strongly enhanced photoluminescence and X-ray excited optical luminescence of the hydrothermally crystallized (Sr, Mn) 5 (PO4) 3 (F, Cl) nanorods by composition modulating. Journal of Alloys and Compounds, 855, 157529.
9. Gao, H., Yu, C., Wang, Y., Wang, S., Yang, H., Wang, F., ... & Li, D. (2022). A novel photoluminescence phenomenon in a $SrMoO_4/SrWO_4$ micro/nano heterojunction phosphors obtained by the polyacrylamide gel method combined with low temperature calcination technology. Journal of Luminescence, 243, 118660.
10. Wang, K., Fu, J., Chang, S., Sun, X., Sun, T., Zhang, S., ... & Tang, M. (2023). Correlating O-deficiency and luminescence property of Tb3+ doped SrO. Advanced Powder Materials, 2(3), 100112.
11. Wang, P., Zhang, W., & Man, S. Q. (2023). Structure, luminescence and energy transfer of Eu^{2+}/ Mn^{2+} co-doped SrO-MgO- B_2O_3 glass for full-color emitting WLEDs. Chemical Physics Letters, 823, 140513.
12. Sharma, S., Kaur, S., Rao, A. S., & Kishor, K. (2023). Thermally stable illuminating characteristics of Tb^{3+}/Sm^{3+} ions activated $BaO–SrO–Al_2O_3–B_2O_3–SiO_2$ glasses for photonic applications. Optical Materials, 145, 114446.
13. Xia, W., Cheng, H., Mao, Q., Ding, Y., Pei, L., Zhu, Y., ... & Zhong, J. (2023). Improving the luminescence performance of far-red-emitting Sr2ScSbO6: Mn4+ phosphor with charge compensation and its application in plant growth LEDs. Ceramics International, 49(9), 13708-13716.
14. El Jouad, M., Touhtouh, S., Sadek, O., & Hajjaji, A. (2022). Structural studies on varied concentrations of europium doped strontium phosphate glasses. Materials Today: Proceedings, 66, 349-352.

15. Guo, H., Zheng, Y., Shi, T., Qin, Z., Zhao, G., Liu, Y., ... & Fang, Y. (2023). Preparation and photoluminescence properties of high thermal stability $Sr_3Ga_2Sn_{1.5}Si_{2.5}O_{14}$: Eu^{3+} red phosphors for high-power light-emitting diodes application. Optical Materials: X, 20, 100264.
16. Kumari, C., Kumar, A., Sharma, S. K., & Manam, J. (2023). Sr3LiSbO6: Er^{3+} phosphors for green LEDs and solar cell applications. Vacuum, 207, 111599.
17. Zhu, G., Li, Z., Zhou, F., Gao, M., Wang, C., & Xin, S. (2019). Novel layered niobate phosphors $SrBaNb_4O_{12}$: Re^{3+} (Re= Eu, Dy, Sm and Pr): crystal structure, electronic Wang, Z., Zhang, M., He, J., Tang, Y., He, T., Sun, Q., ... & Wang, Y. (2021). Strongly enhanced photoluminescence and X-ray excited optical luminescence of the hydrothermally crystallized (Sr, Mn) 5 (PO4) 3 (F, Cl) nanorods by composition modulating. Journal of Alloys and Compounds, 855, 157529.
18. Gao, H., Yu, C., Wang, Y., Wang, S., Yang, H., Wang, F., ... & Li, D. (2022). A novel photoluminescence phenomenon in a $SrMoO_4/SrWO_4$ micro/nano heterojunction phosphors obtained by the polyacrylamide gel method combined with low temperature calcination technology. Journal of Luminescence, 243, 118660.
19. Wang, K., Fu, J., Chang, S., Sun, X., Sun, T., Zhang, S., ... & Tang, M. (2023). Correlating O-deficiency and luminescence property of Tb3+ doped SrO. Advanced Powder Materials, 2(3), 100112.
20. Wang, P., Zhang, W., & Man, S. Q. (2023). Structure, luminescence and energy transfer of Eu^{2+}/ Mn^{2+} co-doped SrO-MgO- B_2O_3 glass for full-color emitting WLEDs. Chemical Physics Letters, 823, 140513.
21. Sharma, S., Kaur, S., Rao, A. S., & Kishor, K. (2023). Thermally stable illuminating characteristics of Tb^{3+}/Sm^{3+} ions activated $BaO–SrO–Al_2O_3–B_2O_3–SiO_2$ glasses for photonic applications. Optical Materials, 145, 114446.
22. Xia, W., Cheng, H., Mao, Q., Ding, Y., Pei, L., Zhu, Y., ... & Zhong, J. (2023). Improving the luminescence performance of far-red-emitting Sr2ScSbO6: Mn4+ phosphor with charge compensation and its application in plant growth LEDs. Ceramics International, 49(9), 13708-13716.
23. El Jouad, M., Touhtouh, S., Sadek, O., & Hajjaji, A. (2022). Structural studies on varied concentrations of europium doped strontium phosphate glasses. Materials Today: Proceedings, 66, 349-352.
24. Guo, H., Zheng, Y., Shi, T., Qin, Z., Zhao, G., Liu, Y., ... & Fang, Y. (2023). Preparation and photoluminescence properties of high thermal stability $Sr_3Ga_2Sn_{1.5}Si_{2.5}O_{14}$: Eu^{3+} red phosphors for high-power light-emitting diodes application. Optical Materials: X, 20, 100264.
25. Kumari, C., Kumar, A., Sharma, S. K., & Manam, J. (2023). Sr3LiSbO6: Er^{3+} phosphors for green LEDs and solar cell applications. Vacuum, 207, 11159.